Electronic Shielding by Closed Shells in Salts of Thulium*

R. G. BARNES
Department of Physics, California Institute of Technology, Pasadena, California
and
Institute for Atomic Research and Department of Physics, Iowa State University, Ames, Iowa

AND

R. L. MÖSSBAUER, E. KANKELEIT, AND J. M. POINDEXTER†
Department of Physics, California Institute of Technology, Pasadena, California
(Received 1 May 1964)

Electronic shielding by closed electron shells has been investigated in salts of trivalent thulium, by measuring the temperature dependence of the nuclear quadrupole splitting of the 8.42-keV gamma transition in Tm^{169}. The measurements were performed by using the technique of recoilless nuclear resonance absorption. The nuclear quadrupole interaction was studied for Tm^{3+} ions in thulium ethyl sulfate, thulium oxide, and thulium trifluoride within a temperature range from 9.6 to 1970°K. The interpretation of the experimental data in terms of the contributions of distorted closed electron shells to the quadrupole interaction yields values for electronic shielding factors. The results lead to amounts of 10% or less for the atomic Sternheimer factor R_Q. The experiments also reveal substantial shielding of the $4f$ electrons from the crystal electric field, expressed by the shielding factor σ_2. Values of 250 and 130 are obtained for the ratio $(1-\gamma_\infty)/(1-\sigma_2)$ for thulium ethyl sulfate and thulium oxide, respectively, where γ_∞ is the lattice Sternheimer factor.

I. INTRODUCTION

MEASUREMENTS of the nuclear quadrupole interaction in salts of the rare-earth elements yield information on the quadrupole moments of the relevant nuclear states and on the electric-field gradients which exist in the salts at the nuclear sites. The extraction of the components of the electric-field gradient tensor from such measurements is rather straightforward if the values of the nuclear quadrupole moments have geen obtained by other methods such as Coulomb excitation techniques. On the other hand, the determination of nuclear moments of rare-earth nuclei by measurements of the nuclear quadrupole interaction is rather involved since this requires a calculation of the components of the electric-field gradient tensor at the nuclear sites. A calculation of the electric-field gradient for salts of the rare earths can be performed at present only with limited accuracy. Uncertainties in excess of 30% are typical. It therefore appears that measurements of the nuclear quadrupole interaction in solids of the rare earths are at present of more importance for studies of the sources of the electric-field gradients than for determination of nuclear quadrupole moments.

The electric-field gradient at the nuclear site of a certain ion originates from a number of different sources. Major sources are distortions of the electronic shells of the ion. These distortions result from the interaction of the electrons of the ion with the crystal electric field (CEF) produced by the surrounding ions in the lattice, provided the arrangement of the surrounding ions reflects a point symmetry lower than cubic. The field gradient at the nuclear site results not only from the distorted partially filled $4f$ electron shell of the rare-earth ion, but also from distorted closed electron shells. These distortions of the closed electron shells of the ion constitute a major source of uncertainty in calculations of the electric field gradient at the nuclear site. The deviations of the closed shells from spherical symmetry (electric multipole polarization) usually lead to substantial reduction or enhancement (shielding or antishielding) of the electric-field gradient at the nuclear site. Sternheimer[1,2] was first to emphasize the importance of magnetic dipole and electric quadrupole polarizations of closed shells and pioneered in calculating the contributions of closed shell deformations to the nuclear hyperfine interactions.

The nuclear quadrupole interaction depends strongly on the electronic state of the ion. The electronic states which arise when a rare-earth ion is incorporated in a crystal lattice are basically caused by the interaction of the CEF and the electrons in the partially filled $4f$ electron shell, but the splittings of these electronic levels are also strongly influenced by distortions of the closed electron shells.[3–5] In order to account for the modification of the CEF splitting which results from electronic shielding, one has to consider the quadrupole moment as well as higher multipole moments induced in the closed shells.

Rare-earth ions exhibit CEF splittings which are usually very much smaller than similar splittings observed for ions of the iron transition elements. In the

* This work was performed under the auspices of the U. S. Atomic Energy Commission, CALT-63-1.
† Participating in the U. S. Navy Graduate Educational Program.

[1] R. M. Sternheimer, Phys. Rev. **80**, 102 (1950); **105**, 158 (1957); R. M. Sternheimer and H. M. Foley, *ibid.* **102**, 731 (1956); H. M. Foley, R. M. Sternheimer, and D. Tyko, *ibid.* **93**, 734 (1954).
[2] R. M. Sternheimer, Phys. Rev. **84**, 244 (1951); **95**, 736 (1954).
[3] D. T. Edmonds, Phys. Rev. Letters **10**, 129 (1963).
[4] R. G. Barnes, E. Kankeleit, R. L. Mössbauer, and J. M. Poindexter, Phys. Rev. Letters **11**, 253 (1963).
[5] J. Blok and D. A. Shirley (private communication).

iron transition series, the partially filled $3d$ electron shell is fully exposed to the CEF produced by surrounding ions, resulting in large CEF level splittings. The relatively small CEF level splittings observed for rare-earth ions, which typically are of the order of a few hundred cm^{-1}, probably arise because of large shielding effects resulting from the $5s^2p^6$ electronic subshell which surrounds the partially filled $4f$ shell.

Present theoretical predictions of the influence of electronic shielding upon the CEF level splitting of rare-earth electronic levels diverge. Burns[6] concluded that electronic shielding in the rare-earth ions is of little importance and that the difference between the CEF level splittings in the iron series and those in the rare-earth series cannot be attributed to electronic shielding of the $4f$ electrons from the CEF by outer closed electron shells. In contrast, Lenander and Wong,[7] Ray,[8] and Watson and Freemen[9] concluded that electronic shielding plays a significant role in rare-earth CEF level splittings.

Quantitative estimates of actual shielding effects are hampered by the lack of sufficiently accurate atomic wave functions for rare-earth ions. Inadequate knowledge of the contributions of the core electrons is a primary source of uncertainty in our present understanding of hyperfine interactions in rare-earth (as well as in other) elements. Direct measurements of the influence of electronic shielding upon the nuclear hyperfine interactions and upon the CEF splittings of electronic levels therefore are highly desirable.

This paper demonstrates the use of the technique of recoilless nuclear resonance absorption of gamma radiation as a means to obtain information on electronic shielding effects in rare-earth isotopes. The procedure introduced here consists of combining measurements of the temperature-dependent nuclear quadrupole interaction (performed by using the technique of recoilless resonance absorption) with measurements of the CEF level splittings (performed by using optical techniques). Specifically we report on determinations of the relevant electronic shielding factors for trivalent thulium based upon our gamma-abosrption measurements of the nuclear quadrupole interaction of Tm^{169} in thulium ethyl sulfate[10] and thulium oxide and on optical measurements of CEF levels by Wong and Richman,[11] Gruber,[12] and Gruber *et al.*[13]

Tm^{169} appeared to be an isotope particularly suited for studies of electronic shielding, for the following major reasons:

(1) The low energy of the 8.4-keV transition used results in a high Debye-Waller factor (recoil-free fraction) even at very high temperatures, thus permitting a measurement of the quadrupole interaction within an unusually wide temperature range.

(2) The separation of the excited levels belonging to the ground multiplet of thulium ($L=6$; $S=1$) is rather large, with the first excited level ($^3H_4$) some 5600 cm^{-1} above the ground term ($^3H_6$). Thus the existence of the higher multiplet levels is of minor concern for the interpretation of our data in thulium, in contrast to the situation prevailing in the case of some other rare-earth ions.

(3) The spin of the nuclear ground state ($I=\frac{1}{2}$) and of the 8.4-keV excited state ($I=\frac{3}{2}$) is rather low, resulting in a small number of quadrupole hyperfine components of the gamma lines which are easily resolvable.

(4) The nuclear collective model applies well to Tm^{169} thus permitting a rather reliable semitheoretical estimate of the nuclear quadrupole moment of the 8.4-keV state.

(5) The relative abundance of Tm^{169} is 100%.

II. CRYSTAL ELECTRIC-FIELD INTERACTIONS

A rare-earth ion interacts in a salt with the CEF produced by all the ions which surround its position in the lattice. The dominant effect is the interaction of the CEF with the electrons in the partially filled $4f$ shell. This interaction is weak compared to the spin-orbit interaction, in contrast with the situation prevailing in the case of iron transition elements. As a result, the total angular momentum **J** remains a good quantum number for rare-earth ions bound in crystals. The effect of the CEF then essentially is a partial or complete removal of the $2J+1$-fold spatial degeneracy of the orientation of **J** which exists in a free ion. The actual number of electronic CEF levels depends on the symmetry of the field, while the level spacing depends on the strength of the interactions between the CEF and the $4f$ electrons. The situation is illustrated in Fig. 1(a).

The potential energy describing the interaction between the CEF and a negative charge at position (r,θ,ϕ) within the ion centered at the origin may be represented in good approximation by the following expansion, not including shielding from closed shells:

$$-eV(r,\theta,\phi)=\sum_{n,}\sum_{m=-n}^{+n}A_n{}^m r^n \Phi_n{}^m(\theta,\phi), \qquad (1)$$

if one assumes that there is no overlap between the charge distributions of different ions. In Eq. (1) the $A_n{}^m$ represent lattice sums over point charges and effective multipole moments in the surrounding ions. The relevant functions $\Phi_n{}^m$, which are linear combina-

[6] G. Burns, Phys. Rev. 128, 2121 (1962).
[7] C. J. Lenander and E. Y. Wong, J. Chem. Phys. 38, 2750 (1963).
[8] D. K. Ray, Proc. Phys. Soc. (London) 82, 47 (1963).
[9] R. E. Watson and A. J. Freeman, Phys. Rev. 133, A1571 (1964).
[10] A preliminary report of part of this work appeared elsewhere (Ref. 4).
[11] E. Y. Wong and I. Richman, J. Chem. Phys. 34, 1182 (1961).
[12] J. B. Gruber and W. F. Krupke (to be published).
[13] J. B. Gruber, W. F. Krupke, and J. M. Poindexter (to be published).

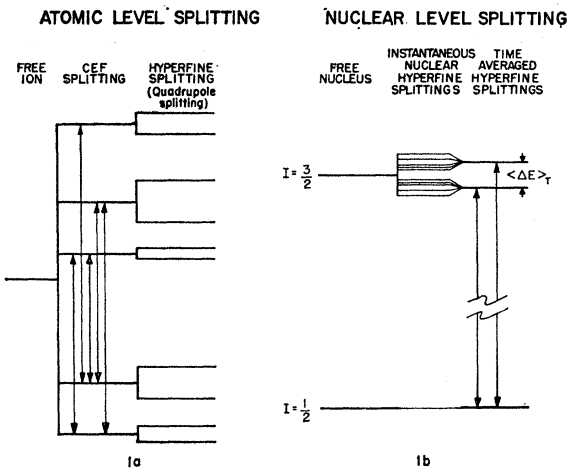

FIG. 1. (a) Schematic of the atomic level splitting of a rare-earth ion in the CEF. For a nuclear spin $I=\frac{3}{2}$ the nuclear quadrupole interaction splits each CEF level into a doublet, which is the case illustrated. Typical over-all CEF splittings are of the order of 10^{-2} eV, while typical quadrupole hyperfine splittings are of the order of 10^{-6} eV. (b) Schematic of the nuclear quadrupole splitting of the 8.4-keV transition in Tm^{169}. The temperature-dependent level splitting $\langle\Delta E\rangle_T$, which is typically of the order of 10^{-6} eV, is the average of the hyperfine splittings of Fig. 1(a), weighted according to their Boltzmann factors.

tions of spherical harmonics $Y_n{}^m$ and $Y_n{}^{-m}$, are defined as follows[14]:

$$\Phi_{2n}{}^0=(2\cdot4\cdot6\cdots2n)P_{2n}(\cos\theta),$$

$$\Phi_n{}^{\pm m}=(2)^m(m!)\frac{(n-m)!}{(n+m)!}P_n{}^m(\cos\theta)\times\begin{Bmatrix}\cos m\phi\\ \sin m\phi\end{Bmatrix},\quad m>0,$$

where P_n and $P_n{}^m$ are Legendre polynomials and associated Legendre functions, respectively. In particular, we obtain for $n=2$:

$$\Phi_2{}^0=3\cos^2\theta-1, \tag{2a}$$

$$\Phi_2{}^2=\sin^2\theta\cos2\phi, \tag{2b}$$

$$\Phi_2{}^{-2}=\sin^2\theta\sin2\phi. \tag{2c}$$

Specifically, the Hamiltonian describing the interaction between the CEF and the electrons in the partially filled $4f$ shell of rare-earth ions, including the effect of shielding via the closed electron shells of the central ion is given by

$$H_{\mathrm{CEF}}{}^{(4f)}=\sum_k\sum_{n,m}A_n{}^m[r_k{}^n+S_n(r_k)]\Phi_n{}^m(\theta_k,\phi_k). \tag{3}$$

The terms proportional to $r_k{}^n$ describe the potential energy due to the direct interaction of the CEF with the kth electron in the $4f$ shell while the terms proportional to $S_n(r_k)$ describe the additional potential energy arising from a deformation of the closed electron shells.

The interaction described by the Hamiltonian in Eq. (3) splits the electronic ground state of the free ion, characterized by total angular momentum **J**, into a number of CEF levels. We shall assume in calculating these CEF levels that the angular and radial parts of the free-ion wave functions can be factorized and that higher terms with different **J** values can be neglected. Under these circumstances we are dealing with a manifold of states belonging to the same **J** and it is then convenient to replace the angular operators occurring in the Hamiltonian, Eq. (3), by equivalent operators.[15] The relevant matrix elements then are of the form

$$H_{m_J,m_J'}=\sum_{n,m}A_n{}^m\langle r^n\rangle_E\langle J\|\theta_n\|J\rangle\times\langle J,m_J|O_n{}^m(J_x,J_y,J_z)|J,m_J'\rangle, \tag{4}$$

where

$$\langle r^n\rangle_E=(1-\sigma_n)\langle r^n\rangle_{4f}, \tag{5}$$

$$\sigma_n=\langle U_{4f}|S_n(r)|U_{4f}\rangle/\langle r^n\rangle_{4f}, \tag{6}$$

$$\langle r^n\rangle_{4f}=\langle U_{4f}|r^n|U_{4f}\rangle, \tag{7}$$

and

$$\theta_n=\alpha,\ \beta,\ \gamma\quad\text{for}\quad n=2,\ 4,\ 6.$$

In these expressions U_{4f} is the radial part of the electronic wave functions for the $4f$ shell. The functions $O_n{}^m(J_x,J_y,J_z)$ are operator equivalents; those relevant for this work are listed in Table I. The expressions $\langle J\|\theta_n\|J\rangle$ are reduced matrix elements,[16] which for the more general case of intermediate coupling are available for Tm^{3+} in the literature.[11–13,17]

It is in principle possible to calculate the parameters $A_n{}^m$ and $\langle r^n\rangle_E$, but difficult in practice. Difficulties arise in the evaluation of the "lattice sums" $A_n{}^m$ because of lack of sufficient knowledge of the ionic position coordinates and their temperature dependence as well as of the values of moments in the surrounding ions.[18] The evaluation of the radial integrals $\langle r^n\rangle_E$, which are the expectation values of r^n for the $4f$ shell modified by contributions from closed shells to the electric multipole fields at the $4f$ electron positions, is hampered by the lack of knowledge of sufficiently accurate atomic wave functions for bound rare-earth ions. For these reasons it is therefore preferable to introduce the "CEF parameters"

$$C_n{}^m=A_n{}^m\langle r^n\rangle_E, \tag{8}$$

to be determined by experiment. The point symmetry of the central ion drastically reduces the number of CEF

[14] The normalization of the functions $\Phi_n{}^m(\theta,\phi)$ is arbitrary; the choice adopted here is the one most commonly used.

[15] K. W. H. Stevens, Proc. Phys. Soc. (London) **A65**, 209 (1952); R. J. Elliott and K. W. H. Stevens, Proc. Roy. Soc. (London) **A218**, 553 (1953); J. P. Elliott, B. R. Judd, and W. A. Runciman, *ibid.* **A240**, 509 (1957); R. Orbach, *ibid.* **A264**, 458 (1961).

[16] B. R. Judd, Proc. Roy. Soc. (London) **A241**, 414 (1957).

[17] J. B. Gruber and J. G. Conway, J. Chem. Phys. **32**, 1531 (1960).

[18] M. T. Hutchings and D. K. Ray, Proc. Phys. Soc. (London) **81**, 663 (1963).

TABLE I. Operator equivalents.

$$O_2^0=3\mathbf{J}_z^2-J(J+1)$$
$$O_2^2=(1/2)[\mathbf{J}_+^2+\mathbf{J}_-^2]$$
$$O_2^{-2}=[1/(2i)][\mathbf{J}_+^2-\mathbf{J}_-^2]$$
$$O_4^0=[35\mathbf{J}_z^4-[30J(J+1)-25]\mathbf{J}_z^2-6J(J+1)+3J^2(J+1)^2]$$
$$O_4^2=(1/4)\{[7\mathbf{J}_z^2-J(J+1)-5]\cdot(\mathbf{J}_+^2+\mathbf{J}_-^2)+(\mathbf{J}_+^2+\mathbf{J}_-^2)\cdot[7\mathbf{J}_z^2-J(J+1)-5]\}$$
$$O_4^{-2}=[1/(4i)]\{[7\mathbf{J}_z^2-J(J+1)-5]\cdot(\mathbf{J}_+^2-\mathbf{J}_-^2)+(\mathbf{J}_+^2-\mathbf{J}_-^2)\cdot[7\mathbf{J}_z^2-J(J+1)-5]\}$$
$$O_4^4=(1/2)[\mathbf{J}_+^4+\mathbf{J}_-^4]$$
$$O_4^{-4}=[1/(2i)][\mathbf{J}_+^4-\mathbf{J}_-^4]$$
$$O_6^0=231\mathbf{J}_z^6-105[3J(J+1)-7]\mathbf{J}_z^4+[105J^2(J+1)^2-525J(J+1)+294]\mathbf{J}_z^2-5J^3(J+1)^3+40J^2(J+1)^2-60J(J+1)$$
$$O_6^2=(1/4)\{[33\mathbf{J}_z^4-\{18J(J+1)+123\}\mathbf{J}_z^2+J^2(J+1)^2+10J(J+1)+102]\cdot(\mathbf{J}_+^2+\mathbf{J}_-^2)$$
$$+(\mathbf{J}_+^2+\mathbf{J}_-^2)\cdot[33\mathbf{J}_z^4-\{18J(J+1)+123\}\mathbf{J}_z^2+J^2(J+1)^2+10J(J+1)+102]\}$$
$$O_6^{-2}=[1/(4i)]\{[33\mathbf{J}_z^4-\{18J(J+1)+123\}\mathbf{J}_z^2+J^2(J+1)^2+10J(J+1)+102]\cdot(\mathbf{J}_+^2-\mathbf{J}_-^2)$$
$$+(\mathbf{J}_+^2-\mathbf{J}_-^2)\cdot[33\mathbf{J}_z^4-\{18J(J+1)+123\}\mathbf{J}_z^2+J^2(J+1)^2+10J(J+1)+102]\}$$
$$O_6^4=(1/4)\{[11\mathbf{J}_z^2-J(J+1)-38]\cdot(\mathbf{J}_+^4+\mathbf{J}_-^4)+(\mathbf{J}_+^4+\mathbf{J}_-^4)\cdot[11\mathbf{J}_z^2-J(J+1)-38]\}$$
$$O_6^{-4}=[1/(4i)]\{[11\mathbf{J}_z^2-J(J+1)-38]\cdot(\mathbf{J}_+^4-\mathbf{J}_-^4)+(\mathbf{J}_+^4-\mathbf{J}_-^4)\cdot[11\mathbf{J}_z^2-J(J+1)-38]\}$$
$$O_6^6=(1/2)(\mathbf{J}_+^6+\mathbf{J}_-^6)$$
$$O_6^{-6}=[1/(2i)](\mathbf{J}_+^6-\mathbf{J}_-^6)$$

parameters.[19] In the case of rare-earth ions only the terms with $n=2$, 4, 6 need to be considered, with the effects of $n=1$, 3, 5 being negligible in most cases.[19]

The wave functions ψ_ν of the νth CEF level will be taken as a linear combination of eigenvectors of the total angular momentum $\mathbf{J}$.

$$\psi_\nu=U(r)\sum_{m_J}a_\nu^{(m_J)}\psi_J^{m_J}. \tag{9}$$

The expansion coefficients $a_\nu^{(m_J)}$ and the energy eigenvalues E_ν follow from the diagonalization of the interaction matrix $H_{m_J,m_J'}$, Eq. (4).

III. THE NUCLEAR QUADRUPOLE INTERACTION

Each of the CEF levels may produce a magnetic field and an electric-field gradient at the nuclear site; this results in hyperfine splittings of the electronic levels. A rare-earth nucleus thus experiences at a certain time a magnetic field and an electric-field gradient which depends on the electronic state that is actually populated at this time. The situation substantially simplifies at elevated temperatures where the spin-lattice relaxation phenomenon produces rapid transitions between the different CEF levels. The nucleus under these circumstances experiences a magnetic field and an electric-field gradient which in essence result from averaging these fields over all electronic states weighted according to the population numbers. This averaging process, which essentially constitutes a time averaging process, holds only if the significant electron relaxation times are short compared to all other relevant times such as the nuclear lifetimes and the nuclear precession times, a situation prevailing at temperatures above a few degrees Kelvin. In particular, the magnetic hyperfine interaction cancels in the absence of an external magnetic field and all one is left with is the quadrupole hyperfine interaction.[20,21] An example of this situation is illustrated in Fig. 1(b) for an assembly of nuclei. The quadrupole interaction is strongly temperature-dependent since the over-all CEF splitting within the lowest electronic term is only of the order of a few hundred cm^{-1}.

The electric-field gradient which interacts with the nuclear quadrupole moment of a rare-earth nucleus bound in an ionic crystal has four significant sources:

(1) One contribution is the direct electric-field gradient produced at the nuclear site by all of the ions surrounding the host ion which contains the nucleus in question. This contribution in the case of rare-earth ions is usually negligible in comparison with the contributions from other sources, particularly at low temperatures.

(2) Another contribution results from the electric-field gradient produced at the nuclear site by the electrons in the partially filled $4f$ shell of the host ion. This field gradient results from the interaction of the $4f$ electrons with the CEF produced by the surrounding ions. This interaction effectively induces electric multipole moments (multipole polarizations) in the $4f$ shell; the quadrupole part of this polarization contributes to the electric-field gradient experienced by the nucleus.

(3) A distortion is usually also induced by the CEF in the closed electron shells, yielding another contribu-

[19] A compilation of the relevant values n and m for various crystal symmetries was given by J. L. Prather, Natl. Bur. Std. (U. S.) Monograph **19**, (1961).

[20] R. L. Cohen, U. Hauser and R. L. Mössbauer, *Proceedings of the Second Mössbauer Conference* (John Wiley & Sons, Inc., New York, 1962), p. 172.

[21] R. L. Mössbauer, Rev. Mod. Phys. **36**, 362 (1964).

tion to the total field gradient experienced by the nucleus. This contribution is proportional to source (1), with proportionality factor $-\gamma_\infty$. The absolute value of the proportionality factor is in the case of the rare earths usually large in comparison with unity, thereby leading to such an enhanced field gradient (antishielding effect) that it often becomes comparable with the one resulting from source (2). This is the "lattice" Sternheimer effect.[22–25]

(4) Another field-gradient contribution due to an induced quadrupole moment in the closed electron shells results from the interaction of the closed electron shells with the electrons in the partially filled $4f$ shell. This relatively small contribution, which is proportional to source (2), with proportionality factor $-R_Q$, is the "atomic" Sternheimer effect.[2,25]

Collecting the different contributions, we obtain for any component $e\mathbf{q}_{ij}$ of the electric-field gradient tensor

$$e\mathbf{q}_{ij}=(1-\gamma_\infty)eq_{ij}^{(\mathrm{Lat})}+(1-R_Q)e\mathbf{q}_{ij}^{(4f)},\ i,j=1,2,3, \quad (10)$$

where γ_∞ and R_Q are the lattice and atomic Sternheimer factors, respectively, as introduced above.

In the principle axes system of the electric-field gradient tensor the nuclear quadrupole interaction Hamiltonian $H_Q^{(\nu)}$ associated with the (ν)th CEF level of the ion is given by

$$\begin{aligned}H_Q^{(\nu)}=\frac{e^2Q}{4I(2I-1)}\{&[(1-R_Q)\langle\nu|\,\mathbf{q}_{zz}^{(4f)}\,|\nu\rangle\\&+(1-\gamma_\infty)q_{zz}^{(\mathrm{Lat})}](3\mathbf{I}_z^2-\mathbf{I}^2)\\&+[(1-R_Q)\langle\nu|\,\mathbf{q}_{xx}^{(4f)}-\mathbf{q}_{yy}^{(4f)}\,|\nu\rangle\\&+(1-\gamma_\infty)(q_{xx}^{(\mathrm{Lat})}-q_{yy}^{(\mathrm{Lat})})]\tfrac{1}{2}(\mathbf{I}_+^2+\mathbf{I}_-^2)\},\end{aligned} \quad (11)$$

where $\mathbf{I}$, $\mathbf{I}_z$, $\mathbf{I}_\pm$ are the usual nuclear spin operators and Q is the nuclear quadrupole moment. The quantities $q_{ii}^{(\mathrm{Lat})}$ and $\langle\nu|\,\mathbf{q}_{ii}^{(4f)}\,|\nu\rangle$ determine the direct contributions to the electric-field gradient at the nuclear site produced by the surrounding ions in the lattice and by the $4f$ electrons of the host ion, respectively. They are defined by

$$eq_{ii}^{(\mathrm{Lat})}=[\partial^2V(r,\theta,\phi)/\partial x_i\partial x_i]_{r=0}, \quad (12)$$

where $V(r,\theta,\phi)$ is defined in Eq. (1), and

$$\langle\nu|\,\mathbf{q}_{ii}^{(4f)}\,|\nu\rangle=\left\langle\nu\left|\sum_k^{4f\ \mathrm{electrons}}\left[\partial^2\left(\frac{-1}{|\mathbf{r}_k-\mathbf{r}|}\right)\Big/\partial x_i\partial x_i\right]_{r=0}\right|\nu\right\rangle, \quad (13)$$

where the wave function $|\nu\rangle$ of the νth CEF level is of the form given by Eq. (9).

[22] E. G. Wikner and G. Burns, Phys. Letters 2, 225 (1969).
[23] D. K. Ray, Proc. Phys. Soc. (London) 82, 47 (1963).
[24] R. M. Sternheimer, Phys. Rev. 132, 1637 (1963).
[25] A. J. Freeman and R. E. Watson, Phys. Rev. 132, 706 (1623).

Explicitly written we obtain for the lattice contribution from Eqs. (1), (2), and (12)

$$e^2q_{zz}^{(\mathrm{Lat})}=-4A_2^0;\ \ e^2(q_{xx}^{(\mathrm{Lat})}-q_{yy}^{(\mathrm{Lat})})=-4A_2^2. \quad (14)$$

Expressing the contributions from the $4f$ electrons within a manifold of states of constant $\mathbf{J}$ in terms of operator equivalents, we obtain from Eq. (13)

$$\langle\nu|\,\mathbf{q}_{zz}^{(4f)}\,|\nu\rangle=-\langle J\|\alpha\|J\rangle\times\langle r^{-3}\rangle_{4f}\langle\nu|\,3\mathbf{J}_z^2-\mathbf{J}^2\,|\nu\rangle, \quad (15a)$$

$$\langle\nu|\,\mathbf{q}_{xx}^{(4f)}-\mathbf{q}_{yy}^{(4f)}\,|\nu\rangle=-(3/2)\langle J\|\alpha\|J\rangle\times\langle r^{-3}\rangle_{4f}\langle\nu|\,\mathbf{J}_+^2+\mathbf{J}_-^2\,|\nu\rangle, \quad (15b)$$

where $\langle r^{-3}\rangle_{4f}$ is defined by Eq. (7). Usually one observes only an average field gradient from the $4f$ electrons, which is a field gradient from the individual CEF levels weighted according to their Boltzmann factors, as discussed above. If we consider only those electronic states which belong to the lowest manifold spanned by the state vector $\mathbf{J}$, then the average direct contribution from the $4f$ electrons to the electric-field gradient acting on the nucleus at temperature T is given by[26]

$$\langle\mathbf{q}_{ii}^{(4f)}\rangle_T=\sum_{\nu=1}^{2J+1}\langle\nu|\,\mathbf{q}_{ii}^{(4f)}\,|\nu\rangle\times\exp(-E_\nu/kT)/\sum_{\nu=1}^{2J+1}\exp(-E_\nu/kT). \quad (16)$$

The diagonal component of the averaged total electric field gradient tensor is according to Eqs. (10) and (16) given by

$$\langle\mathbf{q}_{ii}\rangle_T=(1-\gamma_\infty)q_{ii}^{(\mathrm{Lat})}+(1-R_Q)\langle\mathbf{q}_{ii}^{(4f)}\rangle_T, \quad (17)$$

where we have neglected any temperature dependence of the lattice contribution $q_{ii}^{(\mathrm{Lat})}$.

The total Hamiltonian describing the average quadrupole interaction at temperature T may now according to Eqs. (11) and (17) be written as

$$H_Q(T)=\frac{e^2Q}{4I(2I-1)}[\langle\mathbf{q}_{zz}\rangle_T(3\mathbf{I}_z^2-\mathbf{I}^2)+\langle\mathbf{q}_{xx}-\mathbf{q}_{yy}\rangle_T\tfrac{1}{2}(\mathbf{I}_+^2+\mathbf{I}_-^2)]. \quad (18)$$

We shall now apply the preceding formalism to the particular case of Tm^{169}. The twofold degeneracy of the nuclear ground state of Tm^{169} ($I=\frac{1}{2}$) is not removed by the Hamiltonian (18); the 8.4-keV excited state ($I=\frac{3}{2}$), on the other hand, is split by the nuclear quadrupole interaction into two states. Their energy separation $\langle\Delta E\rangle_T$ which follows from the diagonalization of the Hamiltonian $H_Q(T)$ is given by

$$\langle\Delta E\rangle_T=(e^2Q/2)[\langle\mathbf{q}_{zz}\rangle_T^2+\tfrac{1}{3}\langle\mathbf{q}_{xx}-\mathbf{q}_{yy}\rangle_T^2]^{1/2}. \quad (19)$$

This expression may be written in more detail, by using

[26] A more general description including effects of higher J states is given in the Appendix I.

Eqs. (5), (8), (14), (15), and (17):

$$\langle \Delta E\rangle_T=(e^2Q/2)\left\{\left[\langle J\|\alpha\|J\rangle\langle r^{-3}\rangle_Q\langle 3\mathbf{J}_z^2-\mathbf{J}^2\rangle_T+\frac{4C_2^0}{e^2\langle r^2\rangle_E}(1-\gamma_\infty)\right]^2+\tfrac{1}{3}\left[\tfrac{3}{2}\langle J\|\alpha\|J\rangle\langle r^{-3}\rangle_Q\times\langle \mathbf{J}_+^2+\mathbf{J}_-^2\rangle_T+\frac{4C_2^2}{e^2\langle r^2\rangle_E}(1-\gamma_\infty)\right]^2\right\}^{1/2}, \quad (20)$$

where $\langle 3\mathbf{J}_z^2-\mathbf{J}^2\rangle_T$ and $\langle \mathbf{J}_+^2+\mathbf{J}_-^2\rangle_T$ are thermal averages defined as those given by Eq. (16), while the parameter $\langle r^{-3}\rangle_Q$ is defined by

$$\langle r^{-3}\rangle_Q=(1-R_Q)\langle r^{-3}\rangle_{4f}. \quad (21)$$

It is just this splitting $\langle \Delta E\rangle_T$ that is measured as separation of gamma lines in recoilless resonance absorption experiments.

Several additional hyperfine interaction mechanisms which contribute to the net nuclear quadrupole coupling of a rare-earth ion have been neglected in our calculations. These additional contributions arise in second-order perturbation theory with the principal effects coming from the magnetic hyperfine interaction itself[27] (the so-called pseudoquadrupole coupling) and from the quadrupole interaction with states of higher $\mathbf{J}$ admixed into the ground-state multiplet by the CEF. We have made calculations of these contributions for the compounds covered in this paper and they amount to less than 1% of the total quadrupole interaction energy.

In order to compare experimental results with theory within the framework of the CEF model it is convenient to replace in the theoretical expression for the quadrupole splitting $\langle \Delta E\rangle_T$ all quantities involving electronic radial integrals (the theoretical determinations of which is presently somewhat uncertain) as well as the nuclear quadrupole moment by experimentally observable parameters. For this purpose we introduce the dimensionless parameters

$$\rho_1=e^2Q\langle r^{-3}\rangle_Q\langle J\|\alpha\|J\rangle/C_2^0, \quad (22a)$$

$$\rho_2=Q(1-\gamma_\infty)/\langle r^2\rangle_E. \quad (22b)$$

Expressed in terms of these parameters the quadrupole splitting in Tm^{169} reduces to

$$\langle \Delta E\rangle_T=\tfrac{1}{2}\{[C_2^0\rho_1\langle 3\mathbf{J}_z^2-\mathbf{J}^2\rangle_T+4C_2^0\rho_2]^2+\tfrac{1}{3}[\tfrac{3}{2}C_2^0\rho_1\langle \mathbf{J}_+^2+\mathbf{J}_-^2\rangle_T+4C_2^2\rho_2]^2\}^{+1/2}. \quad (23)$$

The temperature averages $\langle 3\mathbf{J}_z^2-\mathbf{J}^2\rangle_T$ and $\langle \mathbf{J}_+^2+\mathbf{J}_-^2\rangle_T$ within the framework of the CEF model depend only on the experimentally observable CEF parameters C_n^m.

[27] R. J. Elliott, Proc. Phys. Soc. (London) **B70**, 119 (1957).

IV. EXPERIMENTAL TECHNIQUE

The nuclear quadrupole interaction was measured by using the technique of recoilless nuclear resonance absorption of gamma radiation.[28] Measurements of the gamma resonance absorption were performed as a function of the relative velocity between sources and absorbers. The measurements involved sources of erbium trifluoride (ErF_3) and erbium oxide (Er_2O_3) and absorbers of thulium ethyl sulfate ($Tm(C_2H_5SO_4)_3\cdot 9H_2O$) and thulium oxide ($Tm_2O_3$).

Anhydrous ErF_3 provides an excellent source for experiments utilizing the 8.4-keV line of Tm^{169}. The crystal structure of the heavy rare-earth trifluorides has been investigated by Zalkin and Templeton.[29] At temperatures below about 900–1000°C the stable phase is orthorhombic, space group $D_{2h}^{16}-Pnma$, having four formula units per unit cell. The rare-earth ions are crystallographically equivalent, having the point symmetry m. Thus, although the electric-field gradient tensor $e\mathbf{q}_{ij}$ is not axially symmetric, all erbium (or thulium) nuclei experience the same $e\mathbf{q}_{ij}$. According to Eq. (23) the splitting of the recoilless absorption line will approach an asymptotic value for high temperature. In approaching this value it may pass through zero or a minimum at a specific temperature (550°K in the case of ErF_3). The advantages of a single-line source are thereby obtained. The linewidth obtained this way with sources of ErF_3 is less than with sources of Er_2O_3 where the presence of nonequivalent erbium sites complicates the situation.[20,21] At the same time, with reasonable precautions, the ErF_3 can be maintained at the critical temperature for periods of several weeks without decomposition or reaction. This chemical stability does not exist with most other erbium salts in which the erbium ions are also crystallographically equivalent (e.g., the sulfate, nitrate, chloride).

Anhydrous ErF_3 was prepared from erbium metal or erbium oxide by a "wet" process. The metal or oxide was first dissolved in a small quantity of nitric or hydrochloric acid in a polyethylene centrifuge tube. A few mil of aqueous hydrofluoric acid were then added and the mixture heated at approximately 100°C in a water bath for 30 min. The somewhat gelatinous ErF_3 precipitate was then centrifuged down, the excess solution decanted off, the precipitate washed with distilled water, centrifuged three to five times and dried in air at roughly 100°C. Air drying yields a hydrated ErF_3 of unknown composition. To remove the water of hydration, the dry contents of the centrifuge tube bottom were transferred to a small tantalum boat and annealed in an evacuated fused quartz tube. Experience showed that the hydrated ErF_3 could be converted directly into a mixture of the several forms of oxy-

[28] See for instance H. Frauenfelder, *The Mössbauer Effect*, (W. A. Benjamin Inc., New York, 1962).

[29] A. Zalkin and D. H. Templeton, J. Am. Chem. Soc. **75**, 2453 (1953).

fluoride[30] if the annealing temperature was raised too rapidly. The procedure finally adopted was to hold the hydrate at room temperature at about 10^{-5} Torr for at least 12 h in order to pump off most of the water. The temperature was then raised slowly (in 6 h) to 150°C, thus removing virtually all of the water. Finally, the temperature was raised to 850°C in another 6 h and then reduced back to room temperature within 2 h. This procedure yielded consistently good clean x-ray powder patterns of the orthorhombic phase without a trace of the hexagonal phase appearing.[29] ErF_3 prepared in this manner appears to remain stable at room temperature over an indefinite period of time. At elevated temperatures care must be exercised to avoid reaction with oxygen or water vapor. Sources of ErF_3 were prepared in the above manner from Er_2O_3 (usually enriched in Er^{168}) or from erbium metal after irradiation in the Materials Testing Reactor, Arco, Idaho. Alternatively, the ErF_3 was prepared first and then irradiated. Identical spectra were obtained by the two methods.

Absorbers of TmF_3 were used in order to experimentally determine the critical temperature at which the narrowest possible emission line is obtained with sources of ErF_3. Figure 2 shows the temperature dependence of the quadrupole splitting in TmF_3. The source was mounted in a small evacuated oven shown in Fig. 3. The absorber was maintained in a helium atmosphere within an oven equipped with beryllium windows.

It is interesting to note that the same minimum linewidth (1.8 cm/sec) was obtained in both the trifluoride-trifluoride and trifluoride-ethylsulfate experiments. This strongly suggests that the quadrupole splitting of the trifluoride line does indeed pass very near to zero at 550°K.[21]

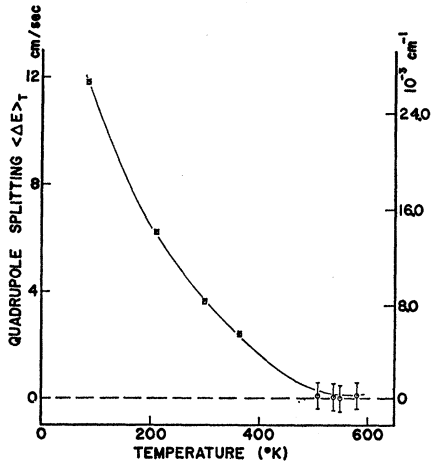

FIG. 2. Temperature dependence of the quadrupole splitting of the 8.4-keV gamma line of Tm^{169} using an ErF_3 source and a TmF_3 absorber. Source and absorber were maintained at the same temperature.

[30] W. H. Zachariasen, Acta Cryst. 4, 231 (1951).

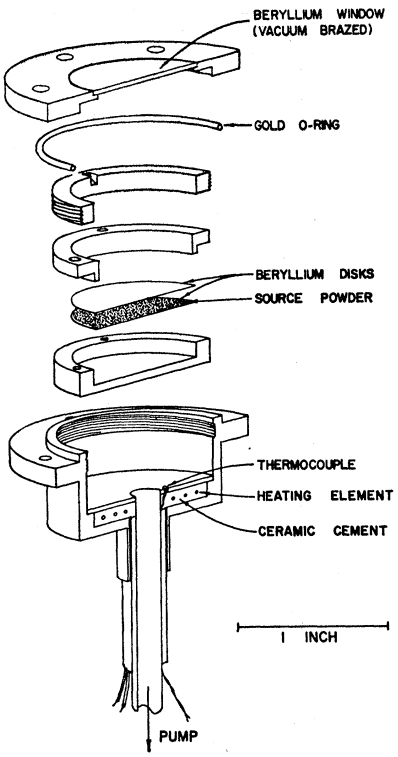

FIG. 3. Details of source oven. The entire oven (weight 200 g) was moved relative to the absorber.

Absorbers of TmES (thulium ethylsulfate) were prepared by crushing single crystals. Absorbers of Tm_2O_3 and sources of (enriched) Er_2O_3 were prepared from commercially available material. Absorbers of all materials to be used below room temperature were prepared by mixing the powdered samples with a soft wax and pressing the mixture into thin disks between mylar films. Absorbers and sources of all materials to be used above room temperature were prepared by settling the powdered samples from a slurry of dry acetone onto $\frac{1}{2}$-mm-thick beryllium windows.

The relative velocities required for Doppler shifting the gamma lines were produced by using both cam drives[31] (providing constant velocities) and transducer drives[32] (providing constant acceleration). Proportional counters filled with one atmosphere of a mixture of 90% argon and 10% methane (by volume) and equipped with $\frac{1}{2}$-mm-thick beryllium windows were used as detectors.

A cryostat specifically designed for recoilless resonance absorption experiments with low-energy gamma radiation was used for the measurements.[33] The sample temperatures in the range from 10 up to 300°K were attained by either controlled heating of the cooled sample holder, by pumping on liquified gases, or by using exchange gas cooling. The sample disks were clamped between thin beryllium disks soldered to the

[31] R. L. Mössbauer, *Proceedings of the Second Mössbauer Conference* (John Wiley & Sons, Inc., New York, 1962), p. 38.
[32] E. Kankeleit, Rev. Sci. Instr. 35, 194 (1964).
[33] F. T. Snively (to be published).

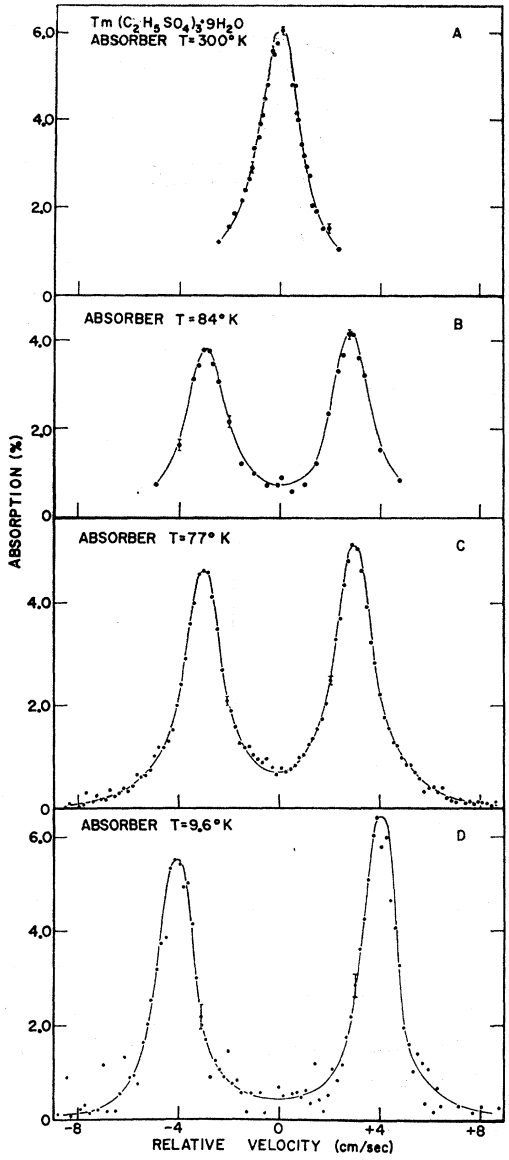

FIG. 4. Quadrupole splitting of the 8.4-keV level of Tm^{169} in an absorber of thulium ethyl sulfate (5 mg/cm² of thulium). A "single line" source of Er^{169} in ErF_3 was used at the critical temperature $T=550°K$ throughout curves *a–d*. The spectra *a*, *b* and *c*, *d* were obtained by using a cam drive and a transducer drive, respectively.

cryostat sample holder in order to ensure good temperature uniformity and stability. Temperature measurements were made using carbon resistors and thermocouples. The ovens used in the measurements above 600°K are described elsewhere.[34]

Some typical spectra are shown in Fig. 4.

V. EXPERIMENTAL RESULTS AND ANALYSIS

The nuclear quadrupole interactions measured as a function of temperature in the compounds TmES and Tm_2O_3 are given in Figs. 5 and 6, respectively. Details of the figures are explained below. The reduction of our experimental results is carried out in two substantially different ways.

[34] J. M. Poindexter, Ph. D. thesis, Department of Physics, California Institute of Technology, Pasadena, 1964 (unpublished).

TABLE II. CEF parameters C_n^m for thulium ethyl sulfate (units cm^{-1}).

Set number	C_2^0	C_4^0	C_6^0	C_6^6	References
1	129.8	−71.0	−28.6	432.8	Wong and Richman, Ref. 11
2	135.2	−71.3	−28.8	428.1	Gruber, Ref. 12
3	130.5	−65.9	−28.6	427.3	See text

Method 1: We combine our nuclear quadrupole splittings obtained from gamma resonance absorption measurements with optically determined CEF levels and obtain the two quantities $\rho_1 C_2^0[(C_2^0)^2+\frac{1}{3}(C_2^2)^2]^{1/2}$ and $\rho_2[(C_2^0)^2+\frac{1}{3}(C_2^2)^2]^{1/2}$ which depend directly on the electronic shielding factors, compare Eqs. (5), (21), and (22). This method emphasizes the low-temperature data, which have the smallest relative errors.

Method 2: The same two quantities may be obtained without the necessity of referring to any optical deter-

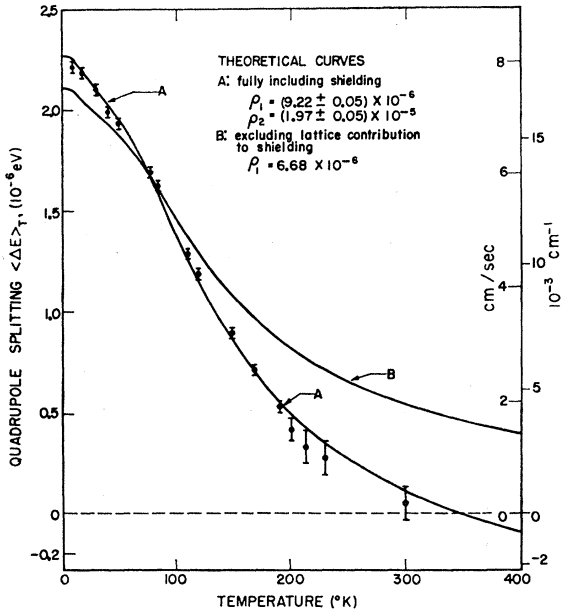

FIG. 5. Temperature dependence of the nuclear quadrupole interaction of Tm^{169} in absorbers of thulium ethyl sulfate (TmES). Sources of ErF_3 ($T=550°K$; single line) were used. Curve A is the best two-parameter fit (parameters ρ_1 and ρ_2) to the experimental data. Curve B is the best one-parameter fit (parameter ρ_1) to the experimental data, thus disregarding the lattice contribution to the electronic shielding (i.e., $\sigma_2=\gamma_\infty=0$). The CEF parameters in set 3 of Table II were used in both curves A and B. Observe that $\langle\Delta E\rangle_{T\to\infty}\to 0$ for curve B.

The difference between curves A and B shows the large contribution of the lattice part $(1-\gamma_\infty)q_{ii}^{(\mathrm{Lat})}$ to the electric-field gradient at the nucleus. Curve B illustrates in particular, that it is not possible to obtain a good fit to the experimental data by merely adjusting the theoretical value of either Q or R_Q.

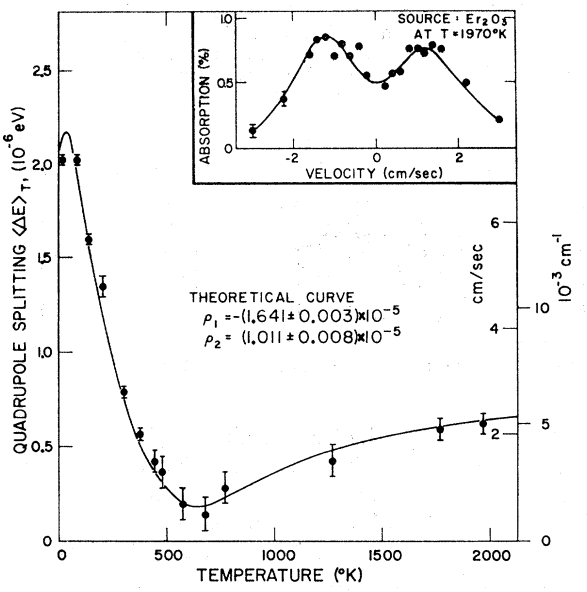

FIG. 6. Temperature dependence of the nuclear quadrupole interaction of Tm^{169} in Tm_2O_3. Sources of ErF_3 ($T=550$°K; single line) and absorbers of Tm_2O_3 (5 mg/cm² of thulium) were used for temperatures of the absorber in the range 11°K<T <700°K. Absorbers of TmES ($T=300$°K; single line; 5 mg/cm² of thulium) and sources of Er_2O_3 were used for temperatures of the source in the range $T>700$°K. The curve is the best two-parameter fit (parameters ρ_1 and ρ_2) to the experimental data using the CEF parameters of Table VI. The insert shows a typical spectrum. The importance of the lattice contribution $(1-\gamma_\infty)\times q_{ii}^{(\mathrm{Lat})}$ to the total field gradient $(1-\gamma_\infty)q_{ii}^{(\mathrm{Lat})}+(1-R_Q)\mathbf{q}_{ii}^{(4f)}$ at the nuclear sites is strikingly demonstrated by the fact, that the quadrupole splitting $\langle\Delta E\rangle_T$ does not approach zero in the high-temperature limit, but rather goes through a minimum and then increases again, with $\langle\mathbf{q}_{ii}\rangle_{T\to\infty}\to(1-\gamma_\infty)q_{ii}^{(\mathrm{Lat})}$.

mination of CEF levels, merely by using gamma resonance measurements obtained at elevated temperatures. This method is useful in those cases where measurements can be performed at temperatures which are large compared to the over-all CEF level splitting, but small compared to the spin-orbit splitting. This is the case in both TmES and Tm_2O_3.

1. Thulium Ethyl Sulfate (TmES)

All rare-earth lattice sites in TmES are occupied by Tm^{3+} ions with point group symmetry C_{3h}. By choosing the proper coordinate system[19] the relevant CEF parameters as defined by Eq. (8) are limited to C_2^0, C_4^0, C_6^0, and C_6^6 for this symmetry. This leads to an axially symmetric electric-field gradient at the nucleus, i.e., $\langle\mathbf{q}_{xx}-\mathbf{q}_{yy}\rangle_T=0$. In this case the quadrupole splitting $\langle\Delta E\rangle_T$ of the gamma lines, Eq. (23), reduces to

$$\langle\Delta E\rangle_T=\tfrac{1}{2}C_2^0[\rho_1\langle 3\mathbf{J}_z^2-\mathbf{J}^2\rangle_T+4\rho_2]. \qquad (24)$$

Method 1: In order to obtain the quantities C_2^0 and $\langle 3\mathbf{J}_z^2-\mathbf{J}^2\rangle_T$ entering in Eq. (24) we use different sets of optically determined CEF parameters given in Table II. Set 1 was obtained for Tm^{3+} in LaES by Wong and Richman,[11] who employed observed optical levels from a series of different optical multiplets. Set 2 was obtained for Tm^{3+} in TmES by Gruber,[12] who again used observed optical levels from a series of different optical multiplets. In contrast, set 3 was obtained by a least-squares method using only levels observed by Gruber[12] in the $^3H_6$ term of Tm^{3+} in TmES. The evaluation of the C_n^m given in set 3 thus does not employ optical terms other than $^3H_6$ and therefore should be the set most appropriate for our reduction of the nuclear quadrupole measurements. To permit a check on the intrinsic consistency obtainable by using one set of CEF parameters for the whole series of optical levels we confront in Table III observed and calculated CEF levels. The over-all agreement is rather encouraging, the average deviations between calculated and observed values being only of the order of experimental uncertainties. Table IV gives for set 3 the wave functions and field gradients for the CEF levels which are necessary for the evaluation of the temperature average $\langle 3\mathbf{J}_z^2-\mathbf{J}^2\rangle_T$, Eqs. (16) and (24).

TABLE III. Observed and calculated CEF levels for thulium ethyl sulfate in the $^3H_6$ term of the ground multiplet (units cm^{-1}). The calculated levels of set 1 were taken from Wong and Richman (Ref. 11). For sets 2 and 3 the following reduced matrix elements were used (Ref. 12): $\langle J\|\alpha\|J\rangle=1.0197\times10^{-2}$, $\langle J\|\beta\|J\rangle=1.5938\times10^{-4}$, and $\langle J\|\gamma\|J\rangle=-5.5318\times10^{-6}$.

Observed levels[a]	Calculated levels[b] Set 1	Set 2	Set 3
302.5	306.8	304.7	300.8
274.0	281.1	279.7	274.3
	219.3	221.2	221.7
	212.9	215.1	215.5
198.9	204.3	204.0	198.8
157.3	162.1	161.4	157.8
110.9	113.3	111.5	110.7
32.1	32.1	28.9	32.0
0	−0.5	−4.4	0.7

[a] Optically determined levels of Gruber (Ref. 12).
[b] Calculated levels using the CEF parameters given in Table II. The center of gravity of the calculated levels is adjusted to give the best fit.

TABLE IV. Energies, wave functions and electric-field gradients of the CEF levels of the $^3H_6$ term of the ground multiplet of thulium ethyl sulfate (C_{3h} symmetry), using the CEF parameters of set 3 and the reduced matrix elements given in the caption of Table III. (Energy in cm^{-1}.)

Energy	Degeneracy	Wave function[a]	$\langle 3\mathbf{J}_z^2-\mathbf{J}^2\rangle$
137.1	1	$-0.707\|-3\rangle+0.707\|+3\rangle$	−15.0
110.6	2	$-0.446\|-2\rangle+0.895\|+4\rangle$	−1.1
		$0.895\|-4\rangle-0.446\|+2\rangle$	
58.0	1	$0.697\|-6\rangle-0.168\|0\rangle+0.697\|+6\rangle$	63.0
51.8	1	$-0.707\|-6\rangle+0.707\|+6\rangle$	66.0
35.1	2	$-0.305\|-1\rangle+0.953\|+5\rangle$	26.3
		$-0.953\|-5\rangle+0.305\|+1\rangle$	
−5.9	1	$0.707\|-3\rangle+0.707\|+3\rangle$	−15.0
−53.0	2	$0.895\|-2\rangle+0.446\|+4\rangle$	−22.9
		$0.446\|-4\rangle+0.895\|+2\rangle$	
−131.7	2	$0.305\|-5\rangle+0.953\|+1\rangle$	−32.3
		$0.953\|-1\rangle+0.305\|+5\rangle$	
−163.0	1	$0.119\|-6\rangle+0.986\|0\rangle+0.119\|+6\rangle$	−39.0

[a] The general form of the wave function is given in Eq. (9).

TABLE V. Reduced data for Tm^{3+} in TmES and in Tm_2O_3. The dimensionless parameters ρ_1 and ρ_2 were obtained in the case of method 1 by a least-squares fit of $\langle \Delta E \rangle_T$, Eq. (23), to the experimental data points given in Figs. 5 and 6. Similarly, in the case of method 2 the parameters ρ_1 and ρ_2 were obtained by fitting Eq. (23) to the experimental data points, using the approximations of Appendix I in the range of their validity, compare Fig. 7. Atomic units are used throughout the table. The errors stated in columns 4 and 5 are only errors arising from our measurements of the nuclear quadrupole interaction and do not include uncertainties in the optical measurements.

Compound	Method	Set	ρ_1	ρ_2	$\langle r^{-3} \rangle_Q$[a]	$(1-\gamma_\infty)/\langle r^2 \rangle_E$[a]
TmES	1	1	$(9.34\pm0.05)\times10^{-6}$	$(2.08\pm0.05)\times10^{-5}$	10.1	390
TmES	1	2	$(9.07\pm0.05)\times10^{-6}$	$(2.17\pm0.05)\times10^{-5}$	10.2	400
TmES	1	3	$(9.22\pm0.05)\times10^{-6}$	$(1.97\pm0.05)\times10^{-5}$	10.0	370
TmES	2	3	$(10\pm3)\times10^{-6}$	$(2.1\pm0.8)\times10^{-5}$	11	390
Tm_2O_3	1	...	$-(1.641\pm0.003)\times10^{-5}$	$(1.011\pm0.008)\times10^{-5}$	11.3	190
Tm_2O_3	2	...	$-(1.7\pm0.9)\times10^{-5}$	$(1.0\pm0.2)\times10^{-5}$	11.6	190

[a] Using the theoretical value $Q=1.5$ b for the nuclear quadrupole moment of the 8.4-keV state of Tm^{169} from M. C. Oleson and B. Elbek [Nucl. Phys. 15, 134 (1960).

A summary of the reduced data obtained by combining our measurements of the temperature dependence of the nuclear quadrupole interaction for Tm^{3+} in TmES with the results of optical measurements performed on the same compound is presented in Table V. The dimensionless parameters ρ_1 and ρ_2 presented in Table V are experimentally obtained quantities (compare Fig. 5, curve A) which hold within the framework of the CEF model. The advantage of introducing these parameters is that their deduction does not depend on a knowledge of the radial distribution of the $4f$ electrons or the value of the nuclear quadrupole moment. Such a knowledge, however, enters into the evaluation of the shielding factors, Eqs. (22), (21), and (5).

Method 2: At elevated temperatures the temperature average $\langle 3\mathbf{J}_z^2-\mathbf{J}^2\rangle_T$ entering in Eq. (24) may be approximated by Eq. (I.17) of Appendix I, which yields $\langle 3\mathbf{J}_z^2-\mathbf{J}^2\rangle_T=-14.1C_2^0/kT$. Expansion (I.17), which applies to the case of an axially symmetric field gradient, was first given by Elliott.[35] Details are given in Appendix I, which also includes an extension to the case of nonaxially symmetric field gradients. From a plot as a function of $1/T$ of our measurements obtained for TmES at temperatures $T>200$°K, Fig. 7, we obtain from Eqs. (24) and (I.17) the values $\rho_1(C_2^0)^2=(0.18\pm0.05)$ cm^{-2} and $\rho_2C_2^0=(2.8\pm1.1)10^{-3}$ cm^{-1}. These values may be compared with the values obtained by method 1: $\rho_1(C_2^0)^2=(0.157\pm0.001)$ cm^{-2} and $\rho_2C_2^0=(2.57\pm0.07)10^{-3}$ cm^{-1}. The agreement between these two values obtained by two different methods gives confidence in the consistency of our analysis. In particular, we conclude on this basis, that our results are not seriously influenced by any temperature dependence of the CEF parameters C_n^m, within the temperature range studied (9.6–300°K). The agreement obtained for the results of methods 1 and 2 indicates that the CEF parameter C_2^0 is reasonably independent of temperature. The justification of the neglect of any temperature dependence of the CEF parameter C_n^m in our analysis is supported by measurements of Gruber and Conway,[36] who determined by optical methods the energies of optical levels of Tm^{3+} ions in TmES at $T=77$, 194, and 273°K. The changes with temperature in the position of the levels typically are less than 10 cm^{-1}. We therefore feel justified in using in our analysis one set of CEF parameters, C_n^m, determined optically at a single temperature.

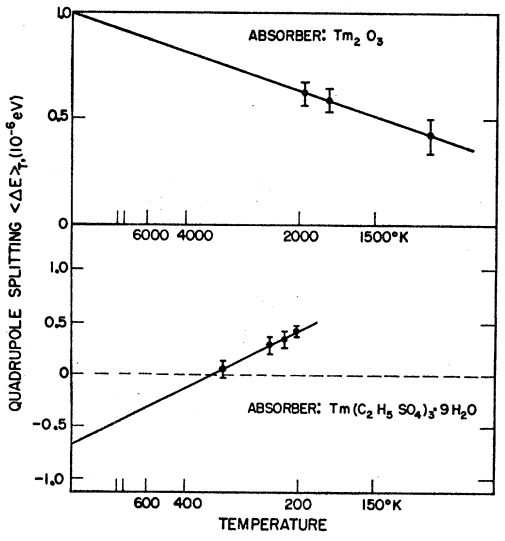

FIG. 7. Nuclear quadrupole interaction of Tm^{169} in absorbers of thulium ethyl sulfate and thulium oxide plotted as a function of $1/T$ in the high-temperature ranges where method 2 is applicable (see text). The straight lines are the best fit to the experimental data points.

2. Thulium Oxide (Tm_2O_3)

The Tm^{3+} ions in the Tm_2O_3 occupy two nonequivalent lattice sites; sites with symmetry C_2 and C_{3i} occur in the ratio 3:1. Experimentally, only the higher populated ionic sites associated with point group symmetry C_2 are observed. By choosing a proper coordinate system[34] the relevant crystal-field parameters for C_2 symmetry are limited to C_2^0, C_2^2, C_4^0, C_4^2, C_4^{-2}, C_4^4, C_4^{-4}, C_6^0, C_6^2, C_6^{-2}, C_6^4, C_6^{-4}, C_6^6, and C_6^{-6}. The

[35] R. J. Elliott, Rev. Mod. Phys. **36**, 385 (1964), and private communication.

[36] J. B. Gruber and J. G. Conway, J. Chem. Phys. **32**, 1178 (1960).

quadrupole splitting of the gamma lines produced by the nonaxially symmetric field gradient is given by Eq. (23).

Method 1: Gruber *et al.*[18] have studied the optical absorption and emission spectra of Tm^{3+} ions in Y_2O_3 at the C_2 symmetry sites; the same CEF levels were obtained in preliminary studies of Tm^{3+} in Tm_2O_3, within the limits of the experimental accuracy. Using the energy levels obtained for diluted Tm^{3+} by Gruber *et al.*,[18] we have calculated the crystal-field parameters C_n^m which are included in Table VI. This calculation was performed by minimizing χ^2, using the technique described by Davidon.[37] A summary of the reduced data obtained by combining our gamma resonance measurements for Tm^{3+} in Tm_2O_3 (compare Fig. 6) with the results of the optical measurements is included in Table V.

Method 2: At elevated temperatures the temperature averages $\langle 3\mathbf{J}_z^2-\mathbf{J}^2\rangle_T$ and $\langle \mathbf{J}_+^2+\mathbf{J}_-^2\rangle_T$ entering in Eq. (23) may in first order be approximated by the expressions given in Eq. (I.17) and (I.18) of Appendix I, which yield $\langle 3\mathbf{J}_z^2-\mathbf{J}^2\rangle_T-14.1C_2^0/kT$ and $\langle \mathbf{J}_+^2+\mathbf{J}_-^2\rangle_T-9.4\,C_2^2/kT$. From a plot as a function of $1/T$ of our measurements obtained for Tm_2O_3 at temperatures $T\geq 1270°K$, Fig. 7, we obtain by using Eqs. (23), (I.17), and (I.18) the following values: $\rho_1 C_2^0[(C_2^0)^2+\frac{1}{3}(C_2^2)^2]^{1/2}=(0.5\pm 0.3)$ cm^{-2} and $\rho_2[(C_2^0)^2+\frac{1}{3}(C_2^2)^2]^{1/2}=(4.0\pm 0.9)10^{-3}$ cm^{-1}. These two values again may be compared with the corresponding values obtained by method 1, namely (0.508 ± 0.001) cm^{-2} and $(3.80\pm 0.03)10^{-3}$ cm^{-1}, respectively. The rather good agreement between the values obtained by methods 1 and 2 suggests, as in the case of TmES, that the neglect in our analysis of any temperature dependence of the CEF parameters C_n^m is a justifiable approximation. Furthermore, the agreement suggests the absence of crystallographic phase transitions in the whole temperature range studied. X-ray diffraction studies of Stecura and Campbell[38] do not reveal any phase transitions within the temperature range $300°K<T<1568°K$.

TABLE VI. Observed and calculated crystal-field levels for Tm^{3+} in thulium oxide at sites with C_2 symmetry, in the $^3H_6$ term of the ground multiplet (units cm^{-1}). The following set of CEF parameters was used[a]: $C_2^0=-82$, $C_2^2=-636$, $C_4^0=-100$, $C_4^2=-1070$, $C_4^{-2}=118$, $C_4^4=837$, $C_4^{-4}=-68$, $C_6^0=3$, $C_6^2=83$, $C_6^{-2}=2$, $C_6^4=227$, $C_6^{-4}=-316$, $C_6^6=1$, $C_6^{-6}=154$.

Calculated levels	Observed[b] levels	Degeneracy	Calculated field gradients $\langle 3J_z^2-J^2\rangle$	$\langle J_+^2+J_-^2\rangle$
770	796.9	1	−1.1	−74.2
768	788.5	1	−4.1	−69.9
680		1	16.8	−43.0
674		1	7.5	−37.9
497	494.0	1	−8.7	42.0
429	435.7	1	−21.3	17.5
344		1	−22.2	−2.3
336	340.0	1	−17.1	25.0
258	230.3	1	−8.3	11.8
200	219.0	1	3.0	22.7
95	89.3	1	−9.9	42.7
44	30.7	1	40.3	28.2
−1	0	1	25.2	37.5

[a] A preliminary set from Gruber *et al.* (Ref. 13).
[b] From Gruber *et al.* (Ref. 13).

[37] W. C. Davidon, Argonne National Laboratory Report ANL-5990 Rev., 1959 (unpublished).

TABLE VII. Theoretical values of Sternheimer shielding factors for rare-earth ions.

Ion	γ_∞	R_{rad}	R_{ang}	Reference
Ce^{3+}	−73.5	−0.43[a]		25
Pr^{3+}	−16.4			8
Pr^{3+}	−105			22
Pr^{3+}	−78.5			24
Tm^{3+}	−61.5			22
Tm^{3+}	−74			24
Eu^{3+}			0.29	2

[a] Using the value (Ref. 25) $\langle r^{-3}\rangle_{4f}=4.71$ a.u.

VI. ELECTRONIC SHIELDING FACTORS

Our experiments reveal the presence of strong charge polarizations of closed electron shells. The shielding (or antishielding) factors R_Q, γ_∞, and σ_2 which were introduced in Secs. II and III, are a measure of these charge polarizations.

The antishielding factor γ_∞ ("lattice" Sternheimer factor) may be calculated by several techniques when the free-ion wave functions are known. Wikner and Burns,[22] Sternheimer,[24] and Freeman and Watson[25] have made calculations of this quantity for certain rare-earth ions, and their results are summarized in Table VII. Wikner and Burns used the (restricted) Hartree-Fock wave functions calculated by Ridley[39] for Pr^{3+} and Tm^{3+} and calculated γ_∞ by means of a perturbation-variation method. Sternheimer used the same wave functions, but calculated γ_∞ by direct solution of the inhomogeneous Schrödinger equation for the perturbed wave functions. Freeman and Watson used the unrestricted Hartree-Fock formalism to calculate γ_∞ for Ce^{3+}. The value of Freeman and Watson for Ce^{3+} is not very different from that obtained by Sternheimer for the neighboring ion Pr^{3+}, but differs appreciably from the value which Wikner and Burns obtained for Pr^{3+}.

Theoretical evaluations of the shielding factor R_Q are more involved. This results because of the proximity of the closed electron shells to the distorting source, the $4f$ electrons. For this reason, one may even expect that the distorted shells may produce repercussions upon the $4f$-electron shell, as was pointed out by Freeman and Watson.[9,40] Table VII includes the few available theoretical values of $R_Q=R_{rad}+R_{ang}$ for rare-earth ions.

[38] S. Stecura and W. J. Campbell, U. S. Bur. Mines, Rept. Invest. No. 5847 (1961).
[39] E. C. Ridley, Proc. Cambridge Phil. Soc. **56**, 41 (1960).
[40] A. J. Freeman and R. E. Watson, Phys. Rev. **131**, 2566 (1963).

TABLE VIII. Semiexperimental electronic shielding factors for trivalent thulium. The values of columns 2 and 6 are taken from Table V. The following theoretical values were used in the table : $\langle r^{-3}\rangle_{4f}=11.20$ from Lindgren[a] (columns 3, 5); $\langle r^2\rangle_{4f}=0.68$ from Judd and Lindgren[b] (column 7); $\langle J\|\alpha\|J\rangle=0.0102$ from several authors (Refs. 11–13, 17) (columns 2, 3); $Q=1.5$ b from Oleson and Elbek[c] (columns 2, 3, 6, 7); $\gamma_\infty=-74$ from Sternheimer (Ref. 24) (columns 6, 7). Atomic units are used throughout the table.

Compound	$\langle r^{-3}\rangle_Q$	R_Q	$\langle r^{-3}\rangle_M$	R_M	$\langle r^2\rangle_E$	σ_2	Reference
TmES[d]	10.0	0.11			0.20	0.71	this paper
Tm_2O_3[e]	11.3	−0.01			0.40	0.41	this paper
Tm Fe_2	9.0[f]	0.20	12.5	−0.12			Cohen[g]
free Tm^3 ion			11.73	−0.05			Gerdau *et al.*[h]

[a] I. Lindgren, Nucl. Phys. **32**, 151 (1962).
[b] B. R. Judd and I. Lindgren, Phys. Rev. **122**, 1802 (1961).
[c] Table V, Ref. a.
[d] Using the data obtained by method 1, set 3.
[e] Using the data obtained by method 1.
[f] Evaluated from Cohen's experimental data, using $Q=1.5$ b.
[g] R. L. Cohen, Phys. Rev. **134**, A94 (1964).
[h] E. Gerdau, W. Krull, L. Mayer, J. Braunsfurth, J. Heisenberg, P. Steiner, and E. Bodenstedt, Z. Physik **174**, 389 (1963).

Theoretical evaluations of the shielding factor σ_2 are physically similar to those for γ_∞. The additional complication arises from the fact, that γ_∞ is a measure of the closed-shell distortions experienced at the origin, while σ_2 is a measure of the closed-shell distortions experienced at the position of the $4f$ electrons, thus requiring in addition a rather precise knowledge of the $4f$-electron density. Theoretical predictions for σ_2 are still rather qualitative. Lenander and Wong[7] came to the conclusion that the shielding factor σ_2 was of the order of 0.5 to 0.75 in the case of $PrCl_3$ while Watson and Freeman[9] in the case of cerium ions likewise conclude that shielding via the σ_2 factor is large. Ray[8] arrives at the theoretical value of $\sigma_2=0.52$ for the case of $PrCl_3$. Burns,[6] on the other hand, using analytic perturbation calculations, concludes that the shielding factor σ_2 should be at most of the order of 0.1 for rare-earth ions.

The analysis of our experimental results yields the parameters ρ_1 and ρ_2 given in Table V. Using the value of the nuclear quadrupole moment Q we can evaluate the parameters $\langle r^{-3}\rangle_Q$ and $(1-\gamma_\infty)/\langle r^2\rangle_E$. Values of these parameters are included in Table V. It appeared reasonable to use a theoretical value for γ_∞ to obtain the radial integral $\langle r^2\rangle_E$, since theoretical evaluations of this quantity appear to be relatively reliable.

Besides the values of the "electric" radial integrals $\langle r^{-3}\rangle_Q$ and $\langle r^2\rangle_E$, which enter in the analysis of our measurements of the nuclear quadrupole interaction, there exists a "magnetic" radial integral $\langle r^{-3}\rangle_M$, which enters in the analysis of nuclear magnetic interactions. The effective integral $\langle r^{-3}\rangle_M$ likewise may be associated with a shielding factor,[2,41] which in analogy with the electric case is defined through the relation $\langle r^{-3}\rangle_M=\langle r^{-3}\rangle_{4f}(1-R_M)$ [compare Eq. (21)]. The difference between the values of $\langle r^{-3}\rangle_Q$ and $\langle r^{-3}\rangle_M$ arises because the contributions from the closed shells differ for the quadrupole and the magnetic interactions. This difference is due to the different forms of the interaction operators for the nuclear quadrupole, magnetic orbital and magnetic spin interactions, as was emphasized by Sternheimer[2,41] and Freeman and Watson.[40]

The radial integrals $\langle r^{-3}\rangle_Q$, $\langle r^{-3}\rangle_M$, and $\langle r^2\rangle_E$, which enter the nuclear quadrupole, nuclear magnetic and CEF interactions, incorporate the contributions to these interactions from both the partially filled ($4f$) and the closed electron shells. These radial integrals in principle may be taken from experimental observations, a procedure adopted in this paper. Table VIII includes a compilation of relevant radial integrals for Tm^{3+} ions in different chemical surroundings, obtained from experimental data by using the theoretical values for Q and γ_∞ given in the caption. The table includes radial integrals evaluated from our gamma resonance studies as well as from other pertinent experiments.

The interpretation of the radial integrals in terms of electronic shielding factors requires a knowledge of the quantities $\langle r^{-3}\rangle_{4f}$ and $\langle r^2\rangle_{4f}$, as discussed above. These radial integrals are not accessible to direct experimental observation and one is forced to use theoretical values, the evaluation of which is presently somewhat uncertain because of the lack of sufficiently accurate atomic wave functions for rare-earth ions. Any evaluation of electronic shielding factors is therefore limited by the uncertainties in these theoretical values. Nevertheless, by using a specific set of theoretical values throughout the whole analysis, one still can observe the general trend in electronic shielding.

Freeman and Watson[42] discuss the theoretical situation in the evaluation of $\langle r^{-3}\rangle_{4f}$ and $\langle r^2\rangle_{4f}$ for most rare-earth ions. These authors, in particular, have shown that the values of $\langle r^{-3}\rangle_{4f}$ for rare-earth ions incorporated in a solid do not differ very much from the free ion values.[25] Table VIII includes a compilation of electronic shielding factors for Tm^{3+} ions obtained by using the theoretical quantities given in the caption. The uncertainties of the theoretical values of Q, $\langle r^2\rangle_{4f}$ and $\langle r^{-3}\rangle_{4f}$ are presumably less than 30%.

It appears from Table VIII that the shielding of the nuclear quadrupole interaction and the nuclear magnetic interaction, expressed through the shielding factors R_Q and R_M, is always small in the case of Tm^{3+} ions.

As concerns shielding factors other than R, we note

[41] R. Sternheimer, Phys. Rev. **86**, 316 (1952).

[42] A. J. Freeman and R. E. Watson, Phys. Rev. **127**, 2058 (1962).

again that our experiments provide only the ratio $(1-\gamma_\infty)/\langle r^2\rangle_B=(1-\gamma_\infty)/[(1-\sigma_2)\langle r^2\rangle_{4f}]$, compare Eqs. (22) and (23). It appears from column 7 of Table VIII that there is a substantial electronic shielding associated with the shielding factor σ_2, which describes the fact that the $4f$ electrons do not interact with the direct CEF, but with a CEF shielded by core electrons (primarily $5s^2p^6$ electrons). This experimental observation is in qualitative agreement with conclusions we draw for praseodymium salts from NMR measurements on lanthanum salts performed by Edmonds.[3] CEF shielding effects of comparable magnitude were also obtained by Blok and Shirley,[5] in the case of several rare-earth ethyl sulfates and rare-earth double nitrates, using nuclear alignment techniques. We note that our conclusions concerning σ_2 are in agreement with the theoretical estimates of Lenander and Wong,[7] Ray,[8] and Watson and Freeman,[9] but are in serious disagreement with theoretical conclusions of Burns.[6]

It is interesting to note the difference in the σ_2 values presented in Table VIII for TmES and Tm_2O_3. This seems to indicate that σ_2 depends on the chemical environment, which might result from different amounts of overlap of ligand wave functions with the central rare-earth ion. This seems to conform with similar conclusions by Hutchings and Ray[18] for the case of $PrCl_3$ and $PrBr_3$. It should be observed that our conclusions concerning σ_2 are based on the plausible assumption that γ_∞ is much less dependent on the chemical bond than σ_2.

Furthermore, we emphasize that we have neglected nonlinear shielding effects[9] in our analysis. Appreciable nonlinear shielding would invalidate the CEF parameterization scheme. However, due to the over-all agreement reached in our analysis—in terms of linear shielding—of the optical data and our quadrupole data, we conclude that nonlinear shielding effects play only a minor role.

Similar measurements of the nuclear quadrupole interaction in TmES to those reported in this paper were performed by Hüfner *et al.*[43] Hüfner *et al.*, in the analysis of their data, did not take into account that the optically determined CEF parameter C_2^0 does not represent an unshielded CEF parameter but rather represents a potential at the $4f$-electron sites which undergoes shielding by closed electron shells of the order of 70%, as shown in this paper. We would like to emphasize, in this context, that the lattice contribution to the total electric-field gradient at the nuclear sites is most easily observed in the measurements performed at higher temperatures.

The nuclear quadrupole interaction in Tm_2O_3 has been investigated previously in a limited temperature range by Cohen *et al.*[20] and Kalvius *et al.*[44] using recoilless resonance absorption of gamma rays. In the analysis of these papers the direct contribution from the lattice to the electric-field gradient, enhanced by electronic shielding, was not considered. Preliminary results for Tm_2O_3 in a limited temperature range were reported by Cohen.[45]

Although the importance of shielding effects expressed by the factor σ_2 is well established, the absolute values of the shielding factor σ_2 may be in error by up to 30%. On these grounds we do not feel that there exists any of the serious discrepancies reported by Hüfner *et al.*[43] between the value of the nuclear quadrupole moments obtained by gamma resonance measurements and those derived from Coulomb excitation measurements.

VII. SUMMARY

This work has demonstrated that the technique of gamma resonance absorption provides a sensitive method for investigating electronic shielding by closed electron shells in rare earths, via measurements of the temperature dependence of the nuclear hyperfine interactions. It was shown, in particular, that in those cases where measurements can be performed at elevated temperatures one can obtain information on electronic shielding factors without the necessity of relying on CEF parameters determined by other methods, such as optical spectroscopy. Our results lead to the conclusion that the distortions induced in the closed electron shells by the $4f$ shell only produce a small shielding of the $4f$-electron contribution to the total field gradient at the nuclear site ("atomic" Sternheimer shielding factor $R_Q\lesssim 0.1$). On the other hand, the distortions induced in the closed electron shells by the CEF lead to substantial enhancement of the direct electric-field gradient produced by the surrounding ions at the nuclear site ("lattice" Sternheimer antishielding factor γ_∞) as well as to a substantial reduction of the CEF as seen by the $4f$ electrons (shielding factor σ_2). We obtain values for $(1-\gamma_\infty)/(1-\sigma_2)$ of 250 for Tm^{3+} ions in thulium ethyl sulfate and of 130 for Tm^{3+} in thulium oxide. The difference in these two values seems to demonstrate a dependence on the chemical bond. It is interesting to note that the ratio of $1-\sigma_2$ for TmES to $1-\sigma_2$ for Tm_2O_3 agrees approximately with the ratio of the over-all CEF splittings in these two compounds.

It appears that measurements of the nuclear quadrupole interaction are presently much better suited to determine electronic shielding factors than to determine nuclear moments, due to the existing uncertainties in the different electronic shielding phenomena.

ACKNOWLEDGMENTS

The authors would like to thank Professor F. H. Spedding for making available the samples of TmES used in this work. It is a pleasure to acknowledge

[43] S. Hüfner, M. Kalvius, P. Kienle, W. Wiedemann, and H. Eicher, Z. Physik **175**, 416 (1963).

[44] M. Kalvius, W. Wiedemann, R. Koch, P. Kienle, and H. Eicher, Z. Physik **170**, 267 (1962).

[45] R. L. Cohen, Ph.D. thesis, Department of Physics, California Institute of Technology, Pasadena, 1962 (unpublished).

stimulating discussions with Dr. R. J. Elliott, Dr. A. J. Freeman, Dr. R. Orbach, Dr. D. A. Shirley, and Dr. E. Y. Wong. We would like to thank Dr. J. B. Gruber for providing us with his optical data prior to publication. We thank F. T. Snively for his participation in part of the measurements. One of us (E.K.) acknowledges the partial support of the Bundesministerium für Wissenschaft of the Federal Republic of Germany. One of us (R.G.B.) gratefully acknowledges the support and hospitality of the California Institute of Technology, which allowed him to participate in this work.

APPENDIX I

In what follows we derive an approximation for the electric-field gradient which holds at elevated temperatures.

The relevant matrix elements entering the expression for the electric-field gradient introduced in the text, Eq. (15), can be expressed in terms of spherical harmonics by

$$\langle J\|\alpha\|J\rangle\langle 3\mathbf{J}_z^2-\mathbf{J}^2\rangle_T = 4(\pi/5)^{1/2}\langle\sum_i \mathbf{Y}_2^0(\vartheta_i,\varphi_i)\rangle_T, \tag{I.1a}$$

$$\langle J\|\alpha\|J\rangle\langle \mathbf{J}_+^2+\mathbf{J}_-^2\rangle_T = 4(2\pi/15)^{1/2}\langle\sum_i[\mathbf{Y}_2^2(\vartheta_i,\varphi_i)+\mathbf{Y}_2^{-2}(\vartheta_i,\varphi_i)]\rangle_T, \tag{I.1b}$$

where the $\sum_i$ extends over all $4f$ electrons.

Using the density matrix formalism the thermal average of the spherical harmonics in Eq. (I.1) may be written as

$$\langle \mathbf{Y}_n^m\rangle_T = Z^{-1}\sum_{\lambda M}\langle\lambda M|\,\mathbf{Y}_n^m \exp[-\beta(H_0+V)]|\lambda M\rangle, \tag{I.2}$$

where

$$Z=\sum_{\lambda M}\langle\lambda M|\exp[-\beta(H_0+V)]|\lambda M\rangle, \tag{I.3}$$

and $\beta=1/kT$. The Coulomb and spin-orbit interactions are represented by H_0 and V is the CEF potential defined by

$$V=\sum_{inm} \mathfrak{A}_n^m r_i^n \mathbf{Y}_n^m(\vartheta_i,\varphi_i), \tag{I.4}$$

and the electronic wave functions $|\lambda\nu\rangle$ for pure Russell-Saunders coupling are defined by

$$(H_0+V)|\lambda\nu\rangle=(E_\lambda+E_\nu)|\lambda\nu\rangle. \tag{I.5}$$

The quantum numbers αLSJ are represented by λ and ν is a quantum number characterizing the CEF levels. Since the trace of a matrix is invariant to the choice of basis functions, we choose eigenfunctions of $\mathbf{J}_z$ in Eqs. (I.2) and (I.3) rather than using the eigenfunctions in Eq. (I.5) which are mixed in M. The "lattice sums" $\mathfrak{A}_n^m$ introduced in Eq. (I.4) are linear functions of those used in the text [compare Eq. (1)]. We have for instance

$$\mathfrak{A}_2^0=4(\pi/5)^{1/2}A_2^0, \tag{I.6a}$$

$$\mathfrak{A}_2^2+\mathfrak{A}_2^{-2}=4(2\pi/15)^{1/2}A_2^2, \tag{I.6b}$$

and we choose $\mathfrak{A}_0^0=0$.

According to Van Hove *et al.*[46] the exponential factor in Eqs. (I.2) and (I.3) may be expanded as follows:

$$\exp[-\beta(H_0+V)]=\sum_{n=0}^{\infty}\rho_n, \tag{I.7}$$

where $\rho_0=\exp(-\beta H_0)$ and for $n>0$ we have

$$\rho_n=(-1)^n\int_0^\beta d\beta_1\int_0^{\beta_1}d\beta_2\cdots\int_0^{\beta_{n-1}}d\beta_n \times\exp[-(\beta-\beta_1)H_0]V\exp[-(\beta_1-\beta_2)H_0]V\cdots \times V\exp[-(\beta_{n-1}-\beta_{n-2})H_0]V\exp(-\beta_n H_0).$$

For a temperature large compared with the CEF interaction energy (i.e., $\beta E_\nu<1$) only the first few terms of Eq. (I.7) need be considered. Hence Eq. (I.2) reduces to

$$\langle \mathbf{Y}_n^m\rangle_T=Z^{-1}\sum_{\lambda\lambda' MM'}\langle\lambda M|\,\mathbf{Y}_n^m|\lambda' M'\rangle \times\langle\lambda' M'|\rho_0+\rho_1+O(\beta^2)|\lambda M\rangle, \tag{I.8}$$

where

$$Z=\sum_{\lambda M}\langle\lambda M|\rho_0+\rho_1+O(\beta^2)|\lambda M\rangle,$$

and

$$\langle\lambda' M'|\rho_0|\lambda M\rangle=\exp(-\beta E_\lambda)\delta_{\lambda\lambda'}\delta_{MM'},$$

$$\langle\lambda' M'|\rho_1|\lambda M\rangle=-\beta\exp(-\beta E_\lambda)\langle\lambda M'|V|\lambda M\rangle \quad \text{for } \lambda=\lambda'$$

$$=-\exp(-\beta E_{\lambda'})\frac{\exp[\beta(E_{\lambda'}-E_\lambda)]-1}{E_{\lambda'}-E_\lambda} \times\langle\lambda' M'|V|\lambda M\rangle \quad \text{for } \lambda\neq\lambda'.$$

Furthermore, if the temperature is also small compared with the spin-orbit splitting (i.e., $\beta(E_{\lambda_1}-E_{\lambda_0})\gg 1$, where λ_1 represents the first excited term of the ground multiplet and λ_0 represents the ground term) only the ground term is appreciably populated. Thus Eq. (I.8) reduces to

$$\langle \mathbf{Y}_n^m\rangle_T=-Z^{-1}\sum_{MM'}[\beta\langle\lambda_0 M|\,\mathbf{Y}_n^m|\lambda_0 M'\rangle\langle\lambda_0 M'|V|\lambda_0 M\rangle +2\sum_{\lambda'\neq\lambda_0}\langle\lambda_0 M|\,\mathbf{Y}_n^m|\lambda' M'\rangle\langle\lambda' M'|V|\lambda_0 M\rangle/E_{\lambda'}], \tag{I.9}$$

for $n>0$. Here $Z=2J_0+1$ and we have chosen $E_{\lambda_0}=0$. Furthermore, because of the Wigner-Eckart theorem and the properties of the vector coupling coefficients

[46] L. Van Hove, N. M. Hugenholtz, and L. P. Howland, *Quantum Theory of Many Particle Systems* (W. A. Benjamin, Inc., New York, 1961), p. 82.

(the notation of Edmond's[47] is used) we have

$$\sum_M \langle \lambda M | \mathbf{Y}_n{}^m | \lambda M \rangle = (2n+1)^{-1/2} \langle \lambda \| \mathbf{Y}_n \| \lambda \rangle \times \sum_M (-1)^{J-M} \langle JMJ-M | JJnm \rangle ,$$

$$(-1)^{J-M} = (2J+1)^{1/2} \langle JMJ-M | JJ00 \rangle ,$$

$$\sum_M \langle JJ00 | JMJ-M \rangle \langle JMJ-M | JJnm \rangle = \delta_{n0}\delta_{m0} ,$$

and therefore

$$\sum_M \langle \lambda M | \mathbf{Y}_n{}^m | \lambda M \rangle = 0 , \quad \text{for} \quad n>0 . \tag{I.10}$$

According to Eq. (I.1) we are only interested in the cases of even n and m, for which we obtain from Eq. (I.9)

$$\langle \mathbf{Y}_n{}^m(\vartheta,\varphi) \rangle_T = -(2J_0+1)^{-1}(2n+1)^{-1} \mathfrak{A}_n{}^{-m} \{ \langle \lambda_0 \| \mathbf{Y}_n(\vartheta) \| \lambda_0 \rangle \sum_i \langle r_i{}^n \rangle \langle \lambda_0 \| \mathbf{Y}_n{}^\dagger(\vartheta_i) \| \lambda_0 \rangle \beta + 2 \sum_{\lambda' \neq \lambda_0} [\langle \lambda_0 \| \mathbf{Y}_n(\vartheta) \| \lambda' \rangle \sum_i \langle r_i{}^n \rangle \langle \lambda' \| \mathbf{Y}_n{}^\dagger(\vartheta_i) \| \lambda_0 \rangle (E_{\lambda'})^{-1}] \} . \tag{I.11}$$

In arriving at Eq. (I.11) we used Eq. (I.4) and the following relations:

$$\sum_{MM'} \langle \lambda_0 M | \mathbf{Y}_n{}^m | \lambda' M' \rangle \langle \lambda' M' | \mathbf{Y}_p{}^q | \lambda_0 M \rangle = [(2n+1)(2p+1)]^{-1/2} \langle \lambda_0 \| \mathbf{Y}_n \| \lambda' \rangle \langle \lambda' \| \mathbf{Y}_p \| \lambda_0 \rangle \sum_{MM'} (-1)^{M+M'} \langle J_0 J' nm | J_0 M J' - M' \rangle \langle J' M' J_0 - M | J' J_0 pq \rangle$$

$$= [(2n+1)(2p+1)]^{-1/2} \langle \lambda_0 \| \mathbf{Y}_n \| \lambda' \rangle \langle \lambda' \| \mathbf{Y}_p \| \lambda_0 \rangle (-1)^m \delta_{np} \delta_{m-q} \Delta(J_0 J' n) ,$$

where $\Delta(J_0 J' n) = 1$ if J_0, J' and n satisfy the triangular condition and Δ is zero otherwise.

Following Elliott and Stevens[15] we now make the following correspondence between reduced matrix elements:

$$\langle J \| \alpha \| J \rangle = 4(\pi/5)^{1/2} \langle \alpha LSJ \| \sum_i \mathbf{Y}_2(\vartheta_i) \| \alpha LSJ \rangle \times (\Omega_{J,J})^{-1/2} , \tag{I.12a}$$

$$\langle J \| \alpha \| J+1 \rangle = -4(\pi/5)^{1/2} \langle \alpha LSJ \| \sum_i \mathbf{Y}_2(\vartheta_i) \| \alpha LSJ+1 \rangle \times (\Omega_{J,J+1})^{-1/2} , \tag{I.12b}$$

$$\langle J \| \alpha \| J+2 \rangle = 4(\pi/5)^{1/2} \langle \alpha LSJ \| \sum_i \mathbf{Y}_2(\vartheta_i) \| \alpha LSJ+2 \rangle \times (\Omega_{J,J+2})^{-1/2} , \tag{I.12c}$$

where

$$\Omega_{J,J} = J(J+1)(2J+1)(2J-1)(2J+3), \tag{I.13a}$$

$$\Omega_{J,J+1} = \tfrac{1}{3} J(J+1)(J+2)(2J+1)(2J+3), \tag{I.13b}$$

$$\Omega_{J,J+2} = \tfrac{2}{3}(J+1)(J+2)(2J+1)(2J+3)(2J+5). \tag{I.13c}$$

Finally, by combining Eqs. (I.1), (I.6), (I.11), and (I.12) we obtain the following expressions:

$$\langle J \| \alpha \| J \rangle \langle 3\mathbf{J}_z{}^2 - \mathbf{J}^2 \rangle_T = A_2{}^0 \langle r^2 \rangle_E \phi(T) , \tag{I.14}$$

$$\langle J \| \alpha \| J \rangle \langle \mathbf{J}_+{}^2 + \mathbf{J}_-{}^2 \rangle_T = \tfrac{2}{3} A_2{}^2 \langle r^2 \rangle_E \phi(T) , \tag{I.15}$$

where

$$\phi(T) = -\tfrac{1}{5}(2J+1)^{-1} \times \left[\frac{|\langle J \| \alpha \| J \rangle|^2 \Omega_{JJ}}{kT} - \frac{2|\langle J \| \alpha \| J\pm1 \rangle|^2 \Omega_{J,J\pm1}}{E_{J\pm1}} + \frac{2|\langle J \| \alpha \| J\pm2 \rangle|^2 \Omega_{J,J\pm2}}{E_{J\pm2}} \right] . \tag{I.16}$$

The factors $\Omega_{J,J-1}$ and $\Omega_{J,J-2}$ in Eq. (I.16) are obtained from Eqs. (I.13b) and (I.13c) by changing J to $J-1$ and $J-2$, respectively. The energies $E_{J\pm1}$ and $E_{J\pm2}$ are those of the center of gravity of the terms nearest the ground term which have quantum numbers $J\pm1$ and $J\pm2$.

Applying these results to the case of Tm^{3+}, the effect of the second and third terms of Eq. (I.16) is negligible ($<1\%$) at all temperatures used in our experiments. Under these circumstances we arrive at the following high-temperature approximations used in method 2 of the text [compare Eqs. (23) and (24)]:

$$\langle 3\mathbf{J}_z{}^2 - \mathbf{J}^2 \rangle_T = -\tfrac{1}{5}(2J+1)^{-1} \times C_2{}^0 \langle J \| \alpha \| J \rangle \Omega_{J,J} (kT)^{-1} , \tag{I.17}$$

$$\langle \mathbf{J}_+{}^2 + \mathbf{J}_-{}^2 \rangle_T = -(2/15)(2J+1)^{-1} \times C_2{}^2 \langle J \| \alpha \| J \rangle \Omega_{J,J} (kT)^{-1} . \tag{I.18}$$

[47] A. R. Edmonds, *Angular Momentum in Quantum Mechanics* (Princeton University Press, Princeton, New Jersey, 1957).